

MicroNewton Force-Controlled Manipulation of Biomaterials Using a Monolithic MEMS Microgripper with Two-Axis Force Feedback

Keekyoung Kim, *Student Member, IEEE*, Xinyu Liu, *Student Member, IEEE*,
Yong Zhang, and Yu Sun, *Senior Member, IEEE*

Abstract—This paper presents the first demonstration of force-controlled micrograsping at the microNewton force level. The system manipulates highly deformable biomaterials (hydrogel microcapsules and biological cells) in an aqueous environment using a MEMS-based microgripper with integrated force feedback along two axes. The microgripper integrates an electrothermal V-beam microactuator and two capacitive force sensors, one for contact detection (force resolution: 38.5nN) and the other for gripping force measurements (force resolution: 19.9nN). The MEMS-based microgripper and the force control system experimentally demonstrate the capability of rapid contact detection and reliable force-controlled micrograsping to accommodate variations in sizes and mechanical properties of objects with a high reproducibility. Cell viability testing validated that the temperature at gripping arm tips does not exceed 50°C.

Index Terms—MEMS microgripper, force control, micrograsping, micro-nanoNewton, biomaterials, microcapsule, cell manipulation.

I. INTRODUCTION

Manipulation of micro- and nanometer-sized objects has found important applications in many areas. For instance, automated microrobotic injection of foreign materials into biological cells greatly facilitates the screening of biomolecules and drug compounds [1], [2]. Manipulation of nanomaterials (e.g., carbon nanotubes and nanoparticles) with AFM [3]–[5] or in SEM (scanning electron microscope) and TEM (transmission electron microscope) [6]–[8] enhances the capability for nano device construction.

Besides visual feedback from optical or electron microscopes, interaction forces between the end-effector and sample under manipulation represent another important form of feedback. Particularly, many objects to be manipulated, such as biomaterials and MEMS (microelectromechanical systems) components are often fragile and prone to damage, necessitating the detection and control of interaction forces in order to avoid sample damage. Employing different types of end-effectors and force sensors, several force-controlled micro- and nanomanipulation systems have been reported [5], [9], [10].

In an AFM-based nanomanipulation system [5], a cantilever probe was used as both an end-effector and a force sensor to conduct force-controlled pushing of nanoparticles on a substrate. Microprobe-based three-dimensional manipulation of microspheres was also reported [9], in which a piezoresistive force sensor was integrated to provide force

The authors are with the Advanced Micro and Nanosystems Laboratory, University of Toronto, 5 King's College Road, Toronto, ON, Canada, M5S 3G8. sun@mie.utoronto.ca

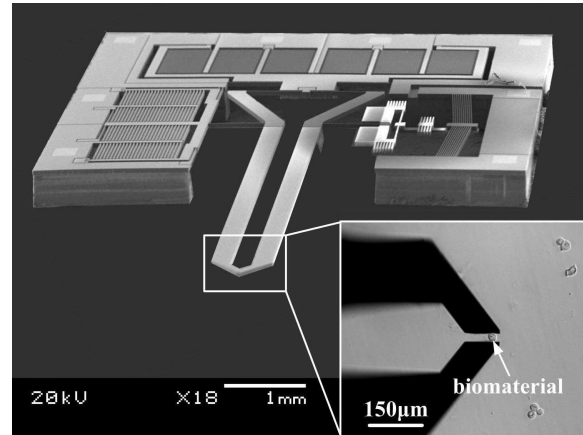


Fig. 1. MEMS-based microgripper with integrated two-axis force sensor. Inlet picture shows microNewton force-controlled grasping of biomaterials.

feedback for a PI (proportional-integral) controller. Although pick-and-place of microspheres was demonstrated in the air by virtue of adhesion forces, the operation reliability/reproducibility was low, which is affected by many factors such as sample type and size, temperature, and humidity. Moreover, pick-and-place using a single probe is only possible in dry or humid (vs. liquid) environments since adhesion forces such as electrostatic force and surface tension would become less significant in an aqueous environment where biomaterials survive [11].

Compared to micro- and nanoprobes with a single end, a microgripper having two gripping arms permits more reliable and controlled manipulation in both air and liquid. A microassembly system using a piezo-driven meso-scaled gripper was developed to assemble micro-parts into three-dimensional structures [10]. Strain gauges were attached to the gripping arms for gripping force measurements. Although this gripper design has a low force sensing resolution (sub-milliNewton), it demonstrated that micrograsping is a viable approach for dexterous micromanipulation tasks. For force-controlled micro- and nanomanipulation, microgrippers should ideally be capable of providing multi-axis force feedback: (1) to protect the microgripper and detect contact between the microgripper and object to be manipulated; and (2) to provide gripping force feedback for achieving secured grasping while protecting the grasped object.

Over the past two decades, continuous efforts have been spent on the design and fabrication of microgrippers based on different mechanical structures and actuation principles [12]–

[20]. Many microgripper designs [12]–[17] focused on material selection, structure synthesis and fabrication, as well as actuator design to achieve large output motions, large gripping forces, and applicability to diverse environments. However, these devices commonly do not have integrated force sensors and thus, cannot perform force-controlled micro- and nanomanipulation.

To address this issue, hybrid microgrippers using piezoresistive or piezoelectric force sensors have been demonstrated, where force sensing components were attached to the gripper structures for detecting gripping forces [18], [19]. The force resolution of hybrid microgrippers is relatively low (tens of microNewtons). Furthermore, manual assembly of force sensors can produce misalignments and cause significant errors in force measurement.

In order to construct monolithic microgrippers with a high force sensing resolution, microfabrication was used to produce microgrippers with on-chip actuators and force sensors in a batch manner. A recently reported monolithic microgripper [20] included an electrostatic microactuator and a capacitive force sensor for measuring gripping forces with a resolution of 70nN. However, no force-controlled micrograsping was demonstrated. The lack of force sensing capabilities along the normal direction for detecting contact forces makes the microgrippers prone to device breakage during manipulation.

This paper presents the first demonstration of force-controlled micrograsping of biomaterials at the microNewton force level, which is conducted with a monolithic MEMS-based microgripper with integrated two-axis force sensors (Fig. 1). The MEMS-based microgripper employs a V-beam electrothermal actuator for generating grasping motions and integrates two-axis differential capacitive force sensors for sensing both gripping forces and contact forces between the gripping arm tips and a sample/substrate. Detection of the contact between the substrate and gripping arm tips is achieved with a microNewton force resolution within seconds. A PID (proportional-integral-derivative) force controller is used to regulate gripping forces for force-controlled micrograsping. The experimental section of the paper presents force-controlled manipulation of micrometer-sized hydrogel microcapsules in liquid, demonstrating that the microgripper and control system are capable of performing robust force-controlled micromanipulation at the microNewton force level.

II. MICROGRIPPER DESIGN, FABRICATION, AND CALIBRATION

Fig. 2(a) shows a schematic of the microgripper design. To grasp an object, V-beam electrothermal actuator is used to control the opening of the active gripping arm. With an applied voltage, the V-beams are heated and thus, expand to produce motion. The shown microgripper is a commonly closed type with an initial opening of $5\mu\text{m}$. When actuated, the active gripping arm is pulled open. In order to prevent a high temperature (e.g., $>50^\circ$) at the gripping arm tips, electrical and thermal insulation on the device silicon layer

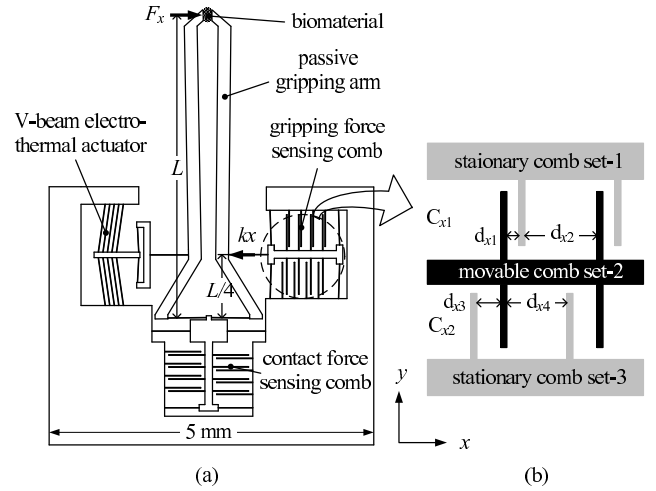


Fig. 2. Device schematics. (a) Microgripper. (b) Differential tri-plate comb drive. The schematic shows a deflected situation.

is implemented and many heat sink beams are used, the effectiveness of which was experimentally verified.

Compared to other types of microactuators such as electrostatic [12], [15], [20], piezoelectric [10], [18], U-beam electrothermal actuators [16], [17], V-beam electrothermal actuators require a much smaller chip area and low driving voltage, produce large forces, and generate large displacements through motion amplification. For the microgrippers reported in this paper, a displacement of $65\mu\text{m}$ is produced with an application of 10V. The much simpler structure of the V-beam actuator (e.g., compared to thousands of comb fingers in electrostatic microgrippers [20]) also significantly helps increase microfabrication yield.

Integrated capacitive force sensors are implemented with transverse differential comb drives and are orthogonally configured. The force sensors enable the measurement of gripping forces as well as contact forces applied at the end of gripping arms along the normal direction (y direction in Fig. 2(a)), both with a resolution of tens of nanoNewton. The gripping force sensor permits secure grasping of an object without applying excessive forces; and the normal force sensor is effective to prevent device breakage when the gripping arms approach a substrate.

Four tethering beams are directly connected to the two gripping arms for transmitting forces. A gripping force (along the x direction) or contact force (along the y direction) respectively deflects four unidirectional sensor springs and further changes comb finger gaps. The total capacitance change resolves an applied force. The eight sensor springs are orthogonally configured to decouple force sensing along the x and y directions. When a gripping force F_x is applied to an object (Fig. 2(a)),

$$F_x L = \frac{kxL}{4} \quad (1)$$

where k is the total spring constant of the four sensor springs, x is the deflection of movable comb fingers, and L is the total length of gripping arms. The four sensor springs are

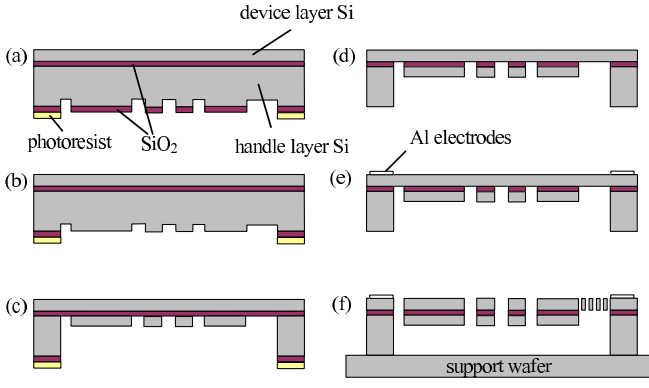


Fig. 3. Microgripper fabrication flow.

modeled as two fixed-fixed beams with a point load applied in the middle. Thus, the spring constant k is

$$k = 4 \frac{Etw^3}{l^3} \quad (2)$$

where $E=100\text{GPa}$ is the average Young's modulus of P-type $\langle 100 \rangle$ silicon, and l , w , and t are spring length, width, and thickness.

In order to achieve a high sensitivity and linear input-output relationship, transverse tri-plate differential comb drives shown in Fig. 2(b) are used [21]. Capacitances are

$$C_{x1} = n \frac{K\varepsilon_0 tl}{d_{x1}} + n \frac{K\varepsilon_0 tl}{d_{x2}}, C_{x2} = n \frac{K\varepsilon_0 tl}{d_{x3}} + n \frac{K\varepsilon_0 tl}{d_{x4}} \quad (3)$$

where K is the dielectric constant for air, ε_0 is the permittivity of free space, $t \times l$ is the overlapping area of comb fingers, and n is the number of comb finger pairs.

By setting $d_{x1} = d_{x3} = 5\mu\text{m} \ll d_{x2} = d_{x4} = 20\mu\text{m}$ in this design, the second term of C_{x1} and C_{x2} becomes negligible. When a gripping force is transmitted to the x directional force sensor, movable comb set-2 in Fig. 2(b) moves away from stationary comb set-3 and closer to stationary comb set-1. The gaps between comb fingers become $d_{x1} = d_0 - x$, $d_{x3} = d_0 + x$. A readout circuit converts capacitance changes into voltages according to

$$V_{out-x} = V_s \left(\frac{C_{x1} - C_{x2}}{C_{x1} + C_{x2}} \right) = V_s \frac{x}{d_0} \quad (4)$$

It can be seen that by placing repeated comb plate units reasonably far apart, a linear sensor input-output relationship can be attained. The above analysis is also applicable to the y direction. Structural-electrostatic coupled finite element simulation was conducted to determine spring dimensions and the placement of comb drives to maximize sensitivity while minimizing cross-axis coupling and nonlinearity.

The microgrippers were fabricated with an SOI wafer with a device layer of $50\mu\text{m}$ using a process modified from [22].

Step a. PECVD (plasma enhanced chemical vapor deposition) SiO_2 on the SOI handle layer. RIE (reactive ion etching) to pattern the PECVD SiO_2 layer. DRIE (deep reactive ion etching) for a depth of $100\mu\text{m}$.

Step b. RIE to remove SiO_2 .

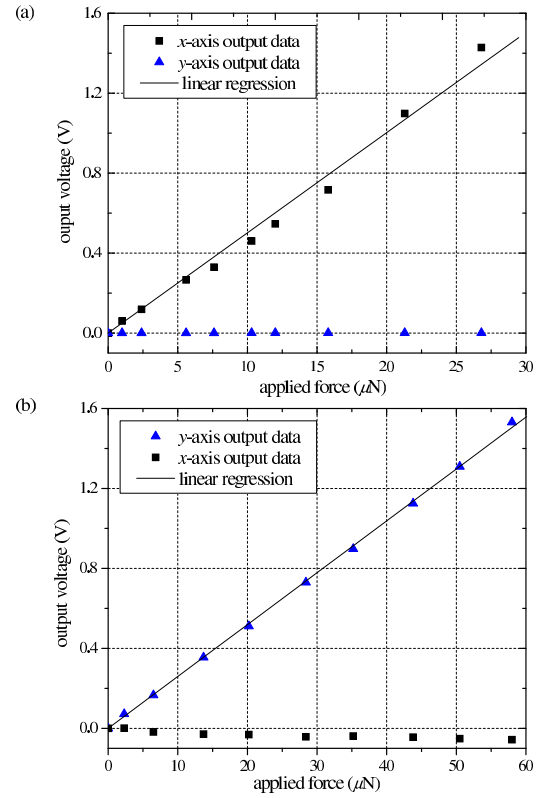


Fig. 4. Force sensor calibration results. Forces applied only (a) along the x direction; (b) only along the y direction. Also shown are coupled responses.

Step c. DRIE etch until the buried SiO_2 layer. This two-step DRIE etching creates a step between the central suspended structure and the device frame, which greatly reduces the risk of device breakage during device operation and handling.

Step d. HF wet etch to remove buried and deposited SiO_2 .

Step e. E-beam evaporate Al and wet etch to form Al electrodes on the device layer.

Step f. DRIE through etch the top device layer to release devices.

The microfabrication process and the use of an SOI wafer permit the creation of electrically insulated but mechanically connected structures as well as effective thermal insulation. Microgrippers were wire-bonded to a custom designed circuit board. The readout circuit was built around an ASIC from Analog Devices (AD7746) for converting capacitance changes into voltage changes.

Force sensor calibration was conducted using a precision microbalance (XS105DU, Mettler Toledo) with a resolution of $0.1\mu\text{N}$. Fig. 4 shows the calibration results of the force sensors along both the x and y directions, proving a linear relationship between applied forces and voltage changes (linearity better than 6%). The microgrippers were calibrated to have a gripping force resolution of 19.9nN and a measurement range of $\pm 50\mu\text{N}$ along the x direction; and a contact force resolution of 38.5nN and a measurement range of $\pm 96\mu\text{N}$ along the y direction.

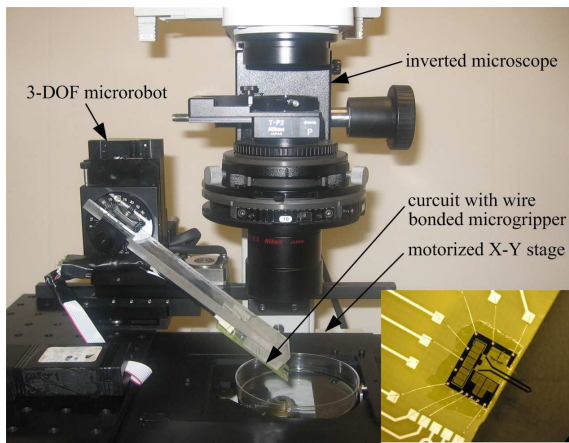


Fig. 5. Force-controlled micromanipulation setup. Inlet picture shows the wire-bonded microgripper.

III. SYSTEM SETUP

The micromanipulation system, as shown in Fig. 5, includes a 3-DOF microrobot (MP-285, Sutter) for positioning the microgripper, a motorized X-Y stage (ProScan II, Prior) for positioning samples, an inverted microscope (TE2000, Nikon) with a CMOS camera (A601f, Basler), a microgripper wire bonded on a circuit board, and a control board (6259, National Instruments) mounted on a host computer. The microgripper was tilted with an angle of 40° to enable the gripping arm tips to reach samples on the substrate without immersing the actuator or force sensors into the liquid medium. All the components except the host computer are mounted on a vibration isolation table.

IV. EXPERIMENTAL RESULTS AND DISCUSSION

Hydrogel microcapsules with 2% chitosan coating for drug delivery were manipulated to demonstrate force-controlled micrograsping. The microcapsules were synthesized using an internal gelation-adsorption-polyelectrolyte coating method [23]. Manipulation/isolation of single microcapsules is required for permeability testing and mechanical property characterization on individual microcapsules.

The experiments were conducted at room temperature (23°C). A droplet of DI water containing suspended microcapsules (ranging from $20\mu\text{m}$ - $40\mu\text{m}$) was dispensed through pipetting on a polystyrene petri dish. After microcapsules settle down on the substrate, the microrobot controls the microgripper to immerse gripping arm tips into the liquid droplet and conducts contact detection.

A. Contact Detection

Contact detection is important to protect the microgripper from damage. After the tips of gripping arms are immersed into the medium, the microrobot controls the microgripper at a constant speed of $20\mu\text{m}/\text{sec}$ to approach the substrate while force data along the y direction are sampled at 90Hz. The contact detection process completes approximately 5sec. Without the integrated contact force sensor, this process

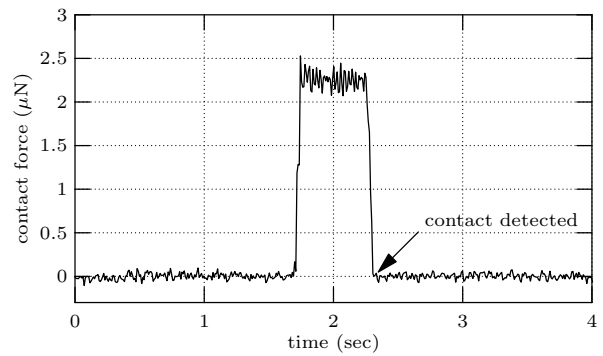


Fig. 6. Contact force monitoring for reliable contact detection.

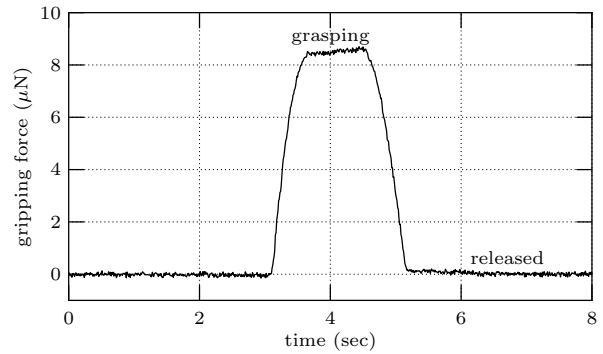


Fig. 8. Gripping force profile during micrograsping and releasing of a microcapsule.

would be extremely time consuming and operator skill dependent.

When the monitored contact force level reaches a pre-set threshold value, it indicates that contact between the gripping arm tips and the substrate is established. Subsequently, the microrobot stops lowering the microgripper further and moves the microgripper upwards until the contact force returns to zero (Fig. 6). After the initial contact position is detected, the microgripper is positioned a few micrometers above the the detected contact position. The pre-set threshold force value used in the experiments was $2.25\mu\text{N}$, which was effective for reliably determining the initial contact between the gripping arm tips and the substrate.

B. Force-Controlled Microcapsule Grasping

Before the system performed force-controlled micrograsping of microcapsules, experiments were conducted to evaluate the effectiveness of open-loop micrograsping. The system applies a voltage to the V-beam electrothermal actuator to produce an opening larger than the size of a microcapsule between the two gripping arms. When grasping a target microcapsule, the system reduces the applied voltage level, which decreases the arm opening and realizes grasping.

Fig. 8 shows a gripping force curve, where a sequence of voltages was applied (5V opening voltage, 1.5V grasping voltage, and 5V releasing voltage) to grasp and release a $25\mu\text{m}$ microcapsule. Due to different sizes of microcapsules and their stiffness variations, a single fixed grasping voltage

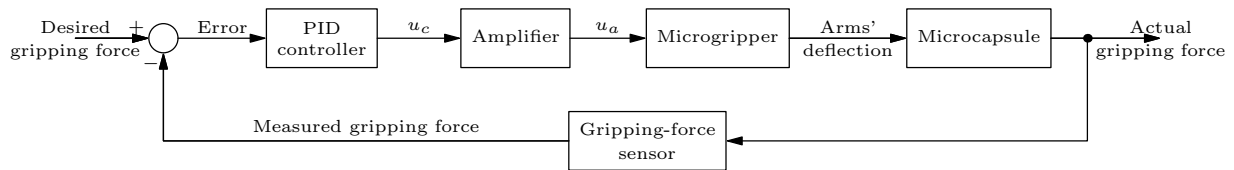


Fig. 7. Block diagram of force-controlled micrograsping.

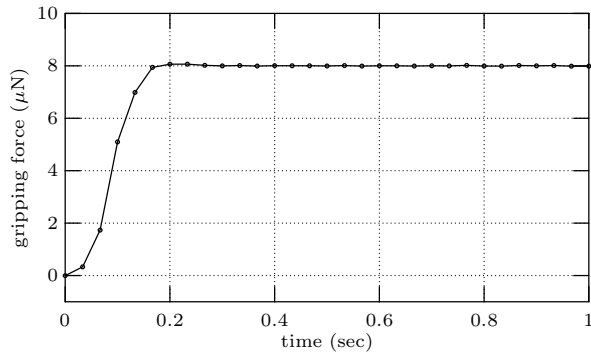


Fig. 9. Step response of force-controlled micrograsping.

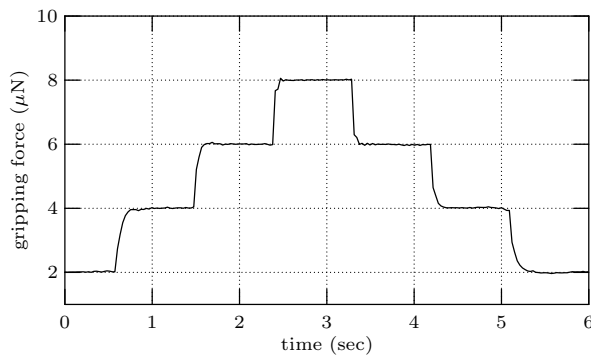


Fig. 10. Tracking force steps with an increment of $2\mu\text{N}$.

can often cause either unsecured grasping or microcapsule breakage due to excessively applied forces, necessitating closed-loop force-controlled micrograsping.

To achieve reliable micrograsping, a closed-loop control system was implemented by using gripping force signals as feedback to form a closed loop. Fig. 7 shows the block diagram of the force control system that accepts a pre-set force level as reference input and employs PID control for force-controlled micrograsping. Fig. 9 shows the step response of the force-controlled micrograsping system to track a reference input of $8\mu\text{N}$. The settling time is approximately 200ms. Corresponding to reference input force steps with an increment of $2\mu\text{N}$, tracking results are shown in Fig. 10.

Enabled by the monolithic microgripper with two-axis force feedback, the system demonstrates the capability of rapidly detecting contact, accurately tracking microNewton gripping forces, and performing reliable force-controlled micrograsping to accommodate size and mechanical property variations of objects. Fig. 11 shows three microcapsules of different sizes that were picked, placed, and aligned.

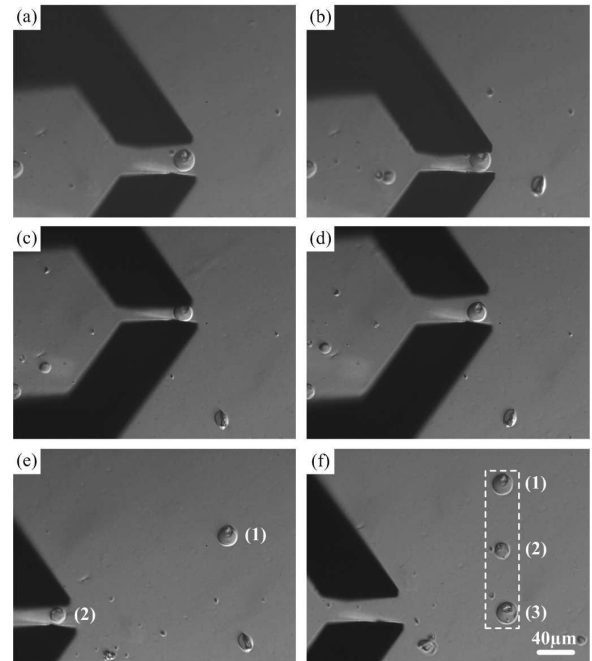


Fig. 11. Microcapsule manipulation and alignment. (a) After contact detection, the opened gripping arms approach a microcapsule. (b) Force-controlled micrograsping. (c) The microgripper transfers the microcapsule to a new position. (d) Releasing the microcapsule. (e) The microgripper leaves the released microcapsule and approaches a second microcapsule. (f) Three microcapsules of different sizes are transferred to desired positions and aligned.

Although the microgripper reveal a gripping force resolution of 19.9nN during sensor calibration, force-controlled micrograsping at a sub-microNewton level proved difficult to achieve. In the micromanipulation environment, the microgripper encounters various noise sources, such as fluidic drag forces, uncontrolled air flow, light emission from the microscope, and electromagnetic interferences from motors of the microrobot and X-Y stage. Due to these noise sources many of which are difficult to model/filter, the microgripper demonstrates a gripping force resolution of $\sim 500\text{nN}$ during micrograsping in liquid. Better circuit shielding and controlled air flow are believed to help alleviate the problem. However, factors such as fluidic drag force effect must be accurately modeled and understood before force-controlled micrograsping of biomaterials at a sub-microNewton level can be realized with a high reproducibility.

C. Cell Grasping for Gripper Arm Temperature Testing

To validate that temperature rise at the gripping arm tips does not exceed a level that biomaterials (e.g., microcapsules

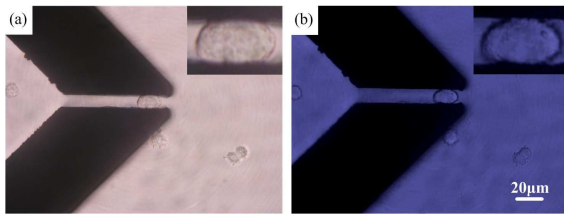


Fig. 12. Micrograsping a porcine aortic valve interstitial cell. (a) The microgripper grasps the cell in cell medium for 2min. (b) Trypan blue was added to the cell medium. After another 10min, the grasped cell remained unstained.

or biological cells) can tolerate, porcine aortic valve interstitial cells (PAVICs) were grasped using the microgripper. A droplet of $100\mu\text{l}$ culture medium containing suspended PAVICs was pipetted on a Petri dish. The microgripper arm tips were immersed into the medium and grasped a cell (Fig. 12(a)). After grasping for 2min, $100\mu\text{l}$ of 0.4% Trypan blue (Invitrogen) solution was added to the medium. The cell was grasped for another 10min to allow sufficient time for complete Trypan blue diffusion and staining. Fig. 12(b) shows that the viability of the cell was not affected by the lengthy micrograsping process. The testing was repeated on five PAVICs, and all cells were proved viable, demonstrating that the temperature at gripping arm tips must not have exceeded 50°C [24].

V. CONCLUSION

Force-controlled micrograsping of highly deformable hydrogel microcapsules at the microNewton force level was demonstrated. The contact force feedback of the MEMS-based microgripper enables the micromanipulation system to conduct rapid contact detection at a microNewton level and protects the microgripper from breakage. The gripping force feedback of the microgripper permits force-controlled micrograsping with a PID force controller to accommodate size and stiffness variations of objects to achieve secured grasping with no excessive forces applied. The temperature rise at the gripping arm tips caused by the integrated electrothermal microactuator was determined to be tolerable by biological cells through cell viability testing. The microgripper and system are suitable for force-controlled micromanipulation of biomaterials in liquid.

VI. ACKNOWLEDGMENT

This work was supported by the Natural Sciences and Engineering Research Council of Canada and by the Ontario Ministry of Research and Innovation. The authors thank Prof. S.X.Y. Wu's group for assisting microcapsule synthesis and Prof. C.A. Simmon's group for interstitial cell preparation.

REFERENCES

- [1] Y. Sun and B. J. Nelson, "Biological cell injection using an autonomous microrobotic system," *Int. J. Robot. Res.*, vol. 21, pp. 861–868, 2002.
- [2] W. H. Wang, X. Y. Liu, D. Gelinias, B. Ciruna, and Y. Sun, "A fully automated robotic system for microinjection of zebrafish embryos," *PLoS ONE*, vol. 2, p. e862, 2007.
- [3] A. A. G. Requicha, "Nanorobots, NEMS, and nanoassembly," *Proc. IEEE*, vol. 91, pp. 1922–1933, 2003.
- [4] H. P. Chen, N. Xi, and G. Y. Li, "CAD-guided automated nanoassembly using atomic force microscopy-based nonrobotics," *IEEE Trans. Auto. Sci. Eng.*, vol. 3, pp. 208–217, 2006.
- [5] M. Sitti and H. Hashimoto, "Controlled pushing of nanoparticles: modeling and experiments," *IEEE Trans. Mech.*, vol. 5, pp. 199–211, 2000.
- [6] L. X. Dong, X. Y. Tao, L. Zhang, X. B. Zhang, and B. J. Nelson, "Nanorobotic spot welding: Controlled metal deposition with attogram precision from copper-filled carbon nanotubes," *Nano Lett.*, vol. 7, pp. 58–69, 2007.
- [7] T. Fukuda, F. Arai, and L. Dong, "Assembly of nanodevices with carbon nanotubes through nanorobotic manipulations," *Proc. IEEE*, vol. 91, pp. 1803–1818, 2003.
- [8] S. Fatikow, T. Wich, H. Hulsen, T. Sievers, and M. Jahnisch, "Microrobot system for automatic nanohandling inside a scanning electron microscope," *IEEE/ASME Trans. Mech.*, vol. 12, pp. 244–252, 2007.
- [9] J. J. Gorman and N. G. Dagalakis, "Probe-based micro-scale manipulation and assembly using force feedback," in *Proc. 1st Joint Emer. Prep. & Response/Robotic & Remote Sys. Top. Mtg.*, Salt Lake City, US, 2006, pp. 621–628.
- [10] J. A. Thompson and R. S. Fearing, "Automating microassembly with ortho-tweezers and force sensing," in *Proc. IEEE/RSJ Int. Conf. Intell. Robot. and Syst.*, Maui, HI, US, 2001, pp. 1327–1334.
- [11] R. S. Fearing, "Survey of sticking effects for micro parts handling," in *Proc. IEEE/RSJ Int. Conf. Intell. Robot. and Syst.*, Pittsburgh, PA, US, 1995, pp. 212–217.
- [12] C.-J. Kim, A. P. Pisano, and R. Muller, "Silicon-processed overhanging microgripper," *J. Microelectromech. Syst.*, vol. 1, pp. 31–36, 1992.
- [13] W. H. Chu and M. Mehregany, "Microfabrication of tweezers with large gripping forces and a large range of motion," in *Proc. Solid-State Sensor and Actuator Workshop*, 1994, pp. 107–110.
- [14] M. Kohl, E. Just, W. Pfleging, and S. Miyazaki, "SMA microgripper with integrated antagonism," *Sens. Actuators A-Phys.*, vol. A83, pp. 1–3, 2000.
- [15] O. Millet, P. Bernardoni, S. Rgnier, P. Bidaud, E. Tsietsiris, D. Collard, and L. Buchailot, "Electrostatic actuated micro gripper using an amplification mechanism," *Sens. Actuators A-Phys.*, vol. 114, pp. 371–378, 2004.
- [16] K. Ivanova, T. Ivanov, A. Badar, B. E. Volland, I. W. Rangelow, D. Andrijašević, F. S. S. Fischer, M. S. W. Brenner, and I. Kostic, "Thermally driven microgripper as a tool for micro assembly," *Microelectron. Eng.*, vol. 83, pp. 1393–1395, 2006.
- [17] N. Chronics and L. P. Lee, "Electrothermally activated SU-8 microgripper for single cell manipulation in solution," *IEEE/ASME J. Microelectromech. Syst.*, vol. 14, pp. 857–863, 2005.
- [18] M. C. Carrozza, A. Eisenberg, A. Menciassi, D. Campolo, S. Micera, and P. Dario, "Towards a force-controlled microgripper for assembling biomedical microdevices," *J. Micromech. Microeng.*, vol. 10, pp. 271–276, 2000.
- [19] D. H. Kim, M. G. Lee, B. Kim, and Y. Sun, "A superelastic alloy microgripper with embedded electromagnetic actuators and piezoelectric force sensors: a numerical and experimental study," *Smart Mater. Struct.*, vol. 3, pp. 208–217, 2006.
- [20] F. Beyeler, A. Neild, S. Oberti, D. J. Bell, Y. Sun, J. Dual, and B. J. Nelson, "Monolithically fabricated microgripper with integrated force sensor for manipulating microobjects and biological cells aligned in an ultrasonic field," *IEEE/ASME J. Microelectromech. Syst.*, vol. 16, pp. 7–15, 2007.
- [21] Y. Sun, S. N. Fry, D. P. Potassek, D. J. Bell, and B. Nelson, "Characterizing fruit fly flight behavior using a microforce sensor with a new comb drive configuration," *IEEE/ASME J. Microelectromech. Syst.*, vol. 14, pp. 4–11, 2005.
- [22] Y. Sun, B. J. Nelson, D. P. Potasek, and E. Enikov, "A bulk microfabricated multi-axis capacitive cellular force sensor using transverse comb drives," *J. Micromech. Microeng.*, vol. 12, pp. 832–840, 2002.
- [23] Q. Liu, A. M. Rauth, and X. Y. Wu, "Immobilization and bioactivity of glucose oxidase in hydrogel microspheres formulated by an emulsification-internal gelation-adsorption-polyelectrolyte coating method," *Int. J. Pharmaceutics*, vol. 14, pp. 4–11, 2005.
- [24] J. Heisterkamp, R. van Hillegersberg, and J. N. IJzermans, "Critical temperature and heating time for coagulation damage: implications for interstitial laser coagulation (ilc) of tumors," *Laser Surg. Med.*, vol. 25, pp. 257–262, 1999.